https://doi.org/10.5194/bg-2020-66
Preprint. Discussion started: 9 April 2020

Biogeosciences Discussions

Silicon isotope fractionation and uptake dynamics of three crop plants: laboratory studies with transient silicon concentrations

Daniel A. Frick[1], Rainer Remus[2], Michael Sommer[2,3], Jürgen Augustin[2], Friedhelm von Blanckenburg[1,4]

[1]GFZ German Research Centre for Geosciences, Potsdam, 14473, Germany.
[2]Leibniz Centre for Agricultural Landscape Research (ZALF), Müncheberg, 15374, Germany.
[3]Institute of Environmental Science and Geography, University of Potsdam, Potsdam, 14476, Germany
[4]Institute of Geological Science, Freie Universität Berlin, Berlin, 12249, Germany.

Correspondence to: Daniel A. Frick (dfrick@gfz-potsdam.de)

Abstract. Silicon has been recognized an important element in global biogeochemical cycles for a long time. Recently, its relevance for global crop production gains increasing attention. Silicon is beneficial for plant growth and is taken up in considerable amounts by crops, likewise rice or wheat. The incorporation of silicic acid from the soil solution into the plants is accomplished by a variety of strategies (rejective, passive and active) that are subject to an intense debate. To forge a new perspective on the underlying processes, we investigated how the silicon stable isotope fractionation during plant growth depends on uptake strategy, transpiration, water use, and Si transfer efficiency. Crop plants with a rejective (tomato, Solanum lycopersicum and mustard, Sinapis alba) and active (spring wheat, Triticum aestivum) uptake were hydroponically grown for 6 weeks. Using inductively coupled plasma mass spectrometry, the silicon amounts and the isotopic composition of the nutrient solution, the roots, and the shoots were determined. Wheat revealed the highest Si transfer efficiency from root to shoot followed by tomato and mustard. All three species preferentially incorporated light ^{28}Si, with a fractionation factor $1000 \cdot \ln(\alpha)$ of -0.33 ‰ (tomato), -0.55 ‰ (mustard) and -0.43 ‰ (wheat). Even though the rates of active and passive Si root uptake differ, the physico-chemical processes governing Si uptake and stable isotope fractionation do not, they are governed by a diffusion process. In contrast, the transport of silicic acid from the roots to the shoots depends on the preceding precipitation of silicic acid in the roots and the presence of active transporters at the root endodermis. Plants with a significant biogenic silica precipitation in roots (mustard, and wheat), preferentially transport silicon enriched in ^{30}Si into their shoots, whereas the transport in tomato is governed by a diffusion process and hence preferentially transports light silicon ^{28}Si into the shoots.

1 Introduction

Silicon (Si) is the second-most abundant element in the Earth's crust and occurs in a wide variety of silicate minerals. Weathering of these minerals mobilises Si, and represents the starting point of Si biogeochemical cycling in terrestrial ecosystems – an often complex web of Si transfers and transformations. One crucial but poorly understood aspect of terrestrial Si biogeochemistry is biological cycling. Si has well documented biological roles, and Si may be recycled multiple times through higher plants before being lost from the system (Carey and Fulweiler, 2012; Derry et al., 2005; Sommer et al., 2006,

https://doi.org/10.5194/bg-2020-66
Preprint. Discussion started: 9 April 2020


Biogeosciences Discussions

2013) Developing and validating geochemical tools to trace plant Si uptake, will improve our ability to answer open questions about weathering, ecosystem nutrition strategies, and geosphere-biosphere interactions.

Despite having a disputed biochemical role, Si is considered beneficial for plant growth, including crops: Si increases abiotic stress mediation (heavy metal sequestration, salinity), biotic stress resistance (defence against herbivores), and improves the plants' structural stability (Coskun et al., 2019; Epstein, 1994, 1999, 2001; Exley and Guerriero, 2019; Ma, 2004; Richmond and Sussman, 2003). Higher plant species can be grouped into three categories depending on the relative amounts of Si taken up: active, passive and rejective (Marschner and Marschner, 2012). Crop plants with an active incorporation mechanism (e.g. rice, and wheat) take up Si with a higher silicon / water ratio than that in the soil solution, thus enriching Si relative to transpired water. Passive uptake plants (most dicotyledons) neither enrich nor deplete the Si relative to the transpired water. Rejective Si uptake plants (e.g. tomato, mustard, and soybean) actively discriminate against Si during uptake (Epstein, 1999; Hodson et al., 2005; Ma et al., 2001; Takahashi et al., 1990). Genome sequencing has uncovered the transporter and mechanism that regulate Si uptake (Ma & Yamaji, 2006; Ma *et al.*, 2006, 2007; Mitani *et al.*, 2009, see also Ma & Yamaji, 2015; YAN *et al.*, 2018 for an overview). In rice, a cooperative system of Si-permeable channels at the root epidermis (called Lsi1, Low Silicon 1 transporter, a thermodynamically passive transporter from the family of aquaporin-like proteins) incorporates Si, whereas a metabolically active efflux transporter (Lsi2, a putative anion-channel transporter) loads Si into the xylem (Broadley et al., 2012). These observations are predictive in nature, and only recently have empirical studies demonstrated the simultaneous operation of passive and active uptake mechanisms (Sun et al., 2016b; YAN et al., 2018). The influence of the different Si transporter and passive Si pathways and their respective relative magnitude on the mobility of silicic acid within plants remains however unknown.

Conventional approaches employed in the study of uptake, translocation, and accumulation of Si in living organisms include either radioactive tracers (e.g. ^{31}Si, ^{32}Si) or homologue elements (e.g. Germanium and the radionuclide ^{68}Ge). Both techniques impose limitations on growth experiments, either due to safety concerns arising from radioactivity or due to physiological differences between the homologue element and Si (Takahashi et al., 1990). As a homologue element, Ge is taken up in the same form as Si, $Ge(OH)_4^0$. In the absence of Si, plants seem to incorporate $Ge(OH)_4$ at a higher rate than in its presence (Takahashi et al., 1990). Several studies have shown that plants fractionate Si relative to Ge, resulting in a lowered Ge/Si ratio in the phytoliths formed (Blecker et al., 2007; Cornelis et al., 2010; Derry et al., 2005; Opfergelt et al., 2010), and there is also evidence that Ge interacts differently with organic molecules than Si (Pokrovski and Schott, 1998; Sparks et al., 2011; Wiche et al., 2018). In some cases, Ge also appears to be toxic to organisms (Marron et al., 2016). Thus, Ge or Ge/Si ratios are problematic tracers of plant Si uptake and translocation processes.

Si stable isotope ratios provide a powerful alternative approach. When combined with measurements of plant physiological properties, they allow exploration of Si cycling in organisms. Each physico-chemical transport process (e.g. absorption, uptake,

https://doi.org/10.5194/bg-2020-66
Preprint. Discussion started: 9 April 2020

diffusion, and precipitation) may be accompanied by a shift in an element's stable isotope ratios - so-called mass-dependent isotope fractionation (Poitrasson, 2017). This isotope fractionation either entails an equilibrium isotope effect, where the isotopes are partitioned between compounds according to bond strength, or a kinetic isotope effect, where the isotope fractionation depends on the relative rate constants of reactions involving the different isotopologues. For stable Si isotope fractionation in aqueous media, both equilibrium effects (He et al., 2016; Stamm et al., 2019) and kinetic effects (Geilert et al., 2014; Oelze et al., 2015; Poitrasson, 2017; Roerdink et al., 2015) have been observed. Previous studies on stable Si fractionation in higher plants focused on rice (Ding et al., 2008a; Köster et al., 2009; Sun et al., 2008, 2016b, 2016a), banana (Delvigne et al., 2009; Opfergelt et al., 2006, 2010), bamboo (Ding et al., 2008b) and cucumber (Sun et al., 2016b) and most of these studies show the preferential incorporation of lighter Si isotopes. Importantly, in most of these studies, Si concentrations in the growth media were held constant by frequently replenishing the nutrient solution. This imparts the disadvantage that the dynamics (temporal evolution) of the Si isotope fractionation during uptake cannot be derived from the isotope shift recorded by the nutrient solution over the course of the experiment, nor does the provision of constant Si amounts allow additional constraints to be placed on Si uptake mechanisms employed by plants.

In this study we elucidated the mechanisms of Si uptake using crop species that differ significantly in their Si uptake capacity and the presence of specific Si transporters. To do so, we combined the measurement of physiological plant performance ratios with observations of the shifts in the Si isotope ratios due to mass dependent isotope fractionation. Three crops - tomato, mustard and wheat - were grown in a hydroponic system, with a finite nutrient supply during the experiment, allowing direct quantification of the dynamics of isotopic fractionation from the temporal evolution of the nutrient solutions' isotopic composition. With the combination of the physiological plant performance ratios and isotope chemical parameters we develop new insights to the mechanisms underlying the different Si uptake and translocation strategies.

2 Materials and Methods

2.1 Nutrient Solution

The nutrient solution was prepared from technical grade salts following the recipe after Schilling *et al.*, 1982; and Mühling & Sattelmacher, 1995. Silicon was added in the form of $NaSiO_4$ to an initial starting concentration of 49.5 $\mu g \cdot g^{-1}$. Details can be found in supplementary methods S1.

2.2 Plant species

Three species were chosen based on their silicon uptake characteristics, the ability to grow in hydroponic environments, and previous knowledge about their Si transporter. Tomato (*Solanum lycopersicum* cultivar MICRO TOM) and mustard (*Sinapis alba*) are both rejective of Si, while spring wheat (*Triticum aestivum* cultivar SW KADRILJ) actively takes up Si (Hodson et al., 2005; Takahashi et al., 1990). The two Si excluder species differ in the presence of the NOD26-like-instrinsic proteins

https://doi.org/10.5194/bg-2020-66
Preprint. Discussion started: 9 April 2020

(orthologues of Lsi1, homologous gene sequence of low silicon rice 1) which are associated with the transport of Si. In the family of Brassicaceae (mustard) these are absent (Sonah et al., 2017), whereas for tomato the Lsi1 homologue seems to be present but inactive (Deshmukh et al., 2016, 2015). Conversely, the alleged active Si efflux transporter (Lsi2-like) are present in the family of Brassicacea (Sonah et al., 2017), but not in tomato.

2.3 Plant germination and growth conditions

Plant seeds were germinated in Petri dishes with half-strength nutrient solution used for the later growth experiment that contained no $NaSiO_4$. After cotyledons formed, seedlings were transferred into a foam block and grown for a further two weeks in the same half-strength nutrient solution. Four plants each were then transferred into one experimental container that was filled with fresh nutrient solution including $NaSiO_4$, and each species was replicated in three containers. Plants were germinated and grown in a growth chamber under controlled climate conditions. Each week the transpired water was replenished with ultrapure water. The temperature in the growth chamber during the day and night was maintained at 18 °C for 14 h and at 15 °C for 10 h, respectively, and the daylight intensity at the top of the container was adjusted to 350 $\mu E \cdot m^{-2} \cdot s^{-1}$) at the start of the experiment. The relative humidity was maintained at approximately 65 %. Details of the plant germination and growth conditions are provided in supplementary methods S2.

2.4 Sampling

The nutrient solutions were sampled at the start of the experiment and then every seven days until harvesting. For sampling, 40 mL were taken after replenishing water loss via transpiration loss and mixing of the solution. All sampled nutrient solutions were stored until analysis in precleaned PP vials in darkness at 4 °C. The 280 mL sample taken over the course of 6 weeks corresponds to 3.5 % of the initial nutrient solution. After 6 weeks the plants were harvested, and stem and leaves were separated from the roots. The roots were immersed multiple times in ultrapure water to remove potential extracellular Si deposits. The plant parts were dried at 104 °C to constant weight.

2.5 Determination of concentrations and isotope ratios

The chemical compositions of the growth solution and the digested plant samples were measured using an axial inductively coupled plasma optical emission spectroscopy (ICP-OES, Varian 720-ES, instrument settings are reported in Table S1). Samples and standard were doped with an excess of $CsNO_3$ (1 mg g^{-1}) to reduce matrix effects that are likely to be caused from the high nitrogen content of the samples. The relative analytical uncertainties are estimated to be below 10% and agreed with the nominal concentration of the starting solutions. For details of the analytical method and an extended verification see ‘S1 Description of analytical methods’ in Schuessler *et al.*, 2016.

https://doi.org/10.5194/bg-2020-66
Preprint. Discussion started: 9 April 2020

2.5.1 Nutrient solution

After the concentration measurements an aliquot of each nutrient solution containing approximately 1000 µg Si was dried down in silver crucibles on a hotplate at 80-95 °C. Crucibles were then filled with a solution containing 400 mg NaOH (prepared from Merck pellets, p.a. grade, previously checked for low Si blank levels) in ultrapure water and dried down. A blank containing ultrapure water and NaOH was processed together with the samples.

2.5.2 Plant samples

The oven-dried samples were homogenised by milling the plant parts in a tungsten carbide planetary ball mill (Pulversiette 7, Fritsch). 50-800 mg of plant material, depending on the estimated Si concentration, was weighed into Ag crucibles and combusted overnight (2h at 200 °C, 4h at 600 °C, then cooled to room temperature) in a furnace (LVT 5/11/P330, Nabertherm). A blank (empty crucible) was processed together with the samples. After cooling the loss of ignition was determined and 400 mg NaOH (TraceSELECT, Sigma-Aldrich) added.

2.5.3 Fusion and chromatography

The crucibles containing the sample (nutrient solution or plant material) and NaOH were placed in a high temperature furnace at 750 °C for 15 min. The fusion cake was dissolved in ultrapure water and 0.03 M HCl, and the pH was adjusted to 1.5. Approximately 60 µg Si was chromatographically separated using cation exchange resin (Georg *et al.*, 2006; Zambardi & Poitrasson, 2011; Schuessler & von Blanckenburg, 2014). The purity and Si yield of the fusion procedure and the column chemistry was determined by ICP-OES. See Methods S3 for more details.

2.5.4 Silicon isotope ratio measurements

The purified solutions were acidified to 0.1 M HCl and diluted to a concentration of 0.6 $\mu g \cdot g^{-1}$. Sample and standard were both doped with 0.6 $\mu g \cdot g^{-1}$ Mg and the $^{25}Mg/^{24}Mg$ ratio used as a monitor of mass bias drift and to ensure stable measurement conditions during the analysis (Oelze et al., 2016). The solutions were introduced using an ESI ApexHF desolvator and a PFA nebuliser (measured uptake 140 µL min^{-1}) into the MC-ICP-MS (Neptune, equipped with the Neptune Plus Jet Interface, Thermo Fisher Scientific; instrument settings are given in Table S1). Measurements were made in dynamic mode (magnet jump) alternating between Si and Mg isotopes, each for 30 cycles with 4 s integration time. ERM-CD281 and BHVO-2 were analysed together with the nutrient and plant samples to ensure complete fusion, dissolution and chromatographic separation. ERM-CD281 resulted in $\delta^{30}Si$ = -0.34 ± 0.20 ‰, 2s, n=13 and BHVO-2 in $\delta^{30}Si$ = -0.29 ± 0.09 ‰, 2s, n=40, in line with literature values. The results of reference materials are reported in the supplementary information in Table S2, and the results of growth solutions and plants in Table S3 and Table S4. All $\delta^{29/28}Si$ and $\delta^{30/28}Si$ are reported in delta notation relative to NBS28 (NIST SRM8546) unless stated otherwise (Coplen et al., 2002; Poitrasson, 2017). An isotopic difference between two compartments is expressed as $\Delta^{30}Si$, calculated following Eq. (1):

https://doi.org/10.5194/bg-2020-66
Preprint. Discussion started: 9 April 2020

$$\Delta^{30}Si_{a-b} = \delta^{30}Si_a - \delta^{30}Si_b \quad (1)$$

where $\delta^{30}Si_a$ is the Si isotopic composition of the compartment a and $\delta^{30}Si_b$ the composition of compartment b. The silicon isotopic composition of a bulk plant is calculated from the mass weighted Si isotopic composition of separate plant parts and expressed as $\delta^{30}Si_{plant}$:

$$\delta^{30}Si_{plant} = \frac{\delta^{30}Si_{root} \cdot M_{root} + \delta^{30}Si_{shoot} \cdot M_{shoot}}{M_{root} + M_{shoot}} \quad (2)$$

where the subscripts plant, root and shoot refer to the bulk plant, and roots and shoots, respectively, and M is the mass of silicon incorporated into the roots or shoots of the plant.

2.6 Plant performance ratios, elemental and isotopic budgets

2.6.1 Plant performance ratios

In order to compare the plant species with respect to their water uptake as well as Si uptake and transfer the following performance ratios were calculated at the end of the experiments:

1. Water use efficiency: total phytomass (g) divided by the amount of transpired water (L), calculated separately for each pot.
2. Si uptake efficiency: total Si mass (mg) in plants divided by the amount of transpired water (L), calculated separately for each pot.
3. Si transfer efficiency: Si mass (mg) in plant shoots divided by the amount of transpired water (L), calculated separately for each pot.

The uptake characteristics were classified based on the ratio of measured and theoretical Si uptake. A ratio of greater than 1 indicates an active uptake mechanism, a ratio much smaller than 1 a rejective strategy, and a ratio of 1 indicates passive uptake. The theoretical Si uptake was calculated based on the amount of transpired water and the nutrient solution Si concentration.

2.6.2 Element budgets

The digested plant samples and nutrient solutions were analysed prior to the column purification by ICP-OES, and the concentrations of major elements (Ca, Fe, K, Mg, P, S and Si) and the retrieval was determined using Eq. (3):

$$Retrieval^X = \frac{M^X_{Solution,end} + M^X_{Plants}}{M^X_{Solution,start}} \; in\,[\%] \quad (3)$$

where $M_{solution,\,end}$ is the mass of the element X in the solution at the end of the experiments, M_{Plants} is the mass of the element X in the plants, and $M_{Solution,\,start}$ the mass of the element X in the solution at the beginning of the experiment.

https://doi.org/10.5194/bg-2020-66
Preprint. Discussion started: 9 April 2020

2.6.2 Silicon isotope budget

A simple test of whether incomplete recovery of Si or analytical artefacts in the Si isotope composition measurements are affecting the results is offered by an isotope budget. The concept is that the summed Si isotope composition of the remaining growth solution at the end of the experiment and the Si taken up by plants should be identical to the Si isotope composition of the initial growth solution. The Si total isotope composition at harvest is estimated using Eq. (4):

$$\delta_{Total} = \frac{M_{solution}^{Si}\delta^{30}Si_{solution} \cdot M_{plants}^{Si}\delta^{30}Si_{plants}}{M_{solution}^{Si}+M_{plants}^{Si}} \quad (4)$$

where $M_{solution}^{Si}$ and M_{plants}^{Si} are the Si amounts in the remaining nutrient solution and the plant parts at harvest, respectively, and $\delta^{30}Si_{solution}$ and $\delta^{30}Si_{plants}$ the Si isotope composition of the remaining nutrient solution and plants parts at the end of the experiment, respectively.

3 Results

3.1 Plant dry mass and transpiration

Substantial differences are apparent in the growth rate between and within all three plant species. During the six-week period mustard formed the greatest amount of dry biomass, with an average of 7 g per plant (range: 0.7 - 16.6 g). Spring wheat produced on average 4 g (range: 1.9 - 5.6 g), and tomato produced the lowest amount of biomass per plant with an average of 3 g (range: 0.2 – 8.7 g, see Table 1 and Table S4 for the individual results). No dependence of replicated growth experiments on pot placement or proximity to the venting system was apparent. The amount of water transpired by the plants during the growth period is correlated with the biomass formed ($r_{Spearman\ Rank}$ = 0.95, p-value <0.001). In contrast, no differences between plant species were observed in terms of the shoot-root ratios (5.4 – 6.5 $g \cdot g^{-1}$, Table 2).

3.2 Dynamics of water, Si and other nutritive elements uptake

The three plant species revealed very different transpiration dynamics during the 6 weeks of plant growth. After a lag phase of two weeks, differences in transpiration between mustard and the other two species became apparent. Figure 1 shows the cumulative transpiration for the three replicate growth experiments and species. Mustard showed the highest, wheat intermediate and tomatoes the lowest cumulative transpiration. The water use efficiency of tomato was significantly higher (3.8 $g \cdot L^{-1}$) than that of the other two plant species (2.4 - 2.6 $g \cdot L^{-1}$, Table 2).

Based on the temporal evolution of Si concentrations in the nutrient solutions (Figure 1) spring wheat exhibited the highest total Si uptake, mustard an intermediate amount, and tomato the lowest total Si uptake and the Si contents of bulk plants reflect this sequence (Table 1): spring wheat as Si accumulator took up the most Si (448 mg), followed by mustard (150 mg). Tomato took up the least amount (95 mg). Considering only roots, the highest Si concentrations and Si amounts were found in mustard,

https://doi.org/10.5194/bg-2020-66
Preprint. Discussion started: 9 April 2020

while spring wheat and tomato were significantly lower. In contrast, considering only plant shoots, the highest Si mass were found in wheat while Si concentrations in mustard and tomato were similar, but more than an order of magnitude lower (Table 1). Spring wheat also showed a much higher Si uptake efficiency than the other two plant species, which resemble each other (Table 2 and Figure 1). The same trend holds for the Si mass ratio between roots and shoots (Table 2). Moreover, wheat shows a much higher efficiency of Si transport into the shoot per mass of transpired water than the other two plant species. In contrast to the Si uptake efficiency, the Si mass ratio between root and shoot for mustard was lower than for tomato (Table 2). For the calculation of Si uptake rates, we assume there is no back diffusion or efflux of Si out of the plant roots. Such a process has not been reported in the literature and would be driven against the concentration difference between the root and the nutrient solution Si concentration and against the water flow direction (Raven, 2001).

After 6 weeks of growth, some nutrients were fully consumed, and the first mustard plants showed signs of deficiency in the form of chlorosis in young and old leaves. Mustard, forming the largest biomass, had also the largest demand for Ca (mean ~644 mg per container), Mg (~140 mg), P (~205 mg) and S (~209 mg). Fig. S1 in the supplement shows the temporal evolution of the other nutrient concentrations for the three plant species.

3.3 Element and Si isotope budgets

The biomass amounts, concentrations, and isotope compositions used to calculate element and Si isotope budgets are reported in the supporting information Table S4. The element retrievals are shown in Table 3. All three plant species showed less than complete retrieval, with variable deficits between elements. For Si the retrieval amounted to between 83% (mustard) and 90% (wheat). For the other nutrients (Ca, Fe, K, Mg, P and S, see Table 3) the retrievals were between 70% and 110%. S in mustard was an exception, with a retrieval of only 50%, which we attribute to the loss of volatile S species during drying and charring, leading to the low retrieval (Blanck et al., 1938). The results for the Si isotope budget are shown in Table 4. Within uncertainty, there is no significant difference between the isotopic composition of the starting solution and the weighted average isotopic composition of the different compartments at the end of the experiment. Thus, we conclude that all significant pathways that fractionate Si isotopes are accounted for.

3.4 Dynamics of isotope fractionation between the nutrient solution and plants

The average initial $\delta^{30}Si$ composition of the nutrient solution is -0.21 ± 0.07 ‰ (2 s, relative to NBS28; individual results are reported in Table S3). The temporal evolution of the nutrient solution and the individual Si isotopic composition of the roots, shoots and the entire plants are shown in Figure 2 (reported as $\Delta^{30}Si$ relative to the nutrient solution). All three plant species preferentially incorporated the lighter silicon isotope (^{28}Si), leaving the nutrient solution enriched in heavier silicon (^{30}Si). After an initial lag phase for all three species, in which the nutrient solution's Si isotope composition does not vary, its isotopic composition becomes increasingly enriched in ^{30}Si. Tomato and mustard, as rejective Si taxa, took up only about 10% of the Si predicted by water transpiration rates over the course of the experiment (Fig. 1; Table 2), such that the enrichment of the

https://doi.org/10.5194/bg-2020-66
Preprint. Discussion started: 9 April 2020

Biogeosciences Discussions Open Access EGU

nutrient solution in ^{30}Si was relatively small ($^{Tomato}\Delta^{30}Si_{Solution:End-Start}$=+0.13 ‰, $^{Mustard}\Delta^{30}Si_{Solution:End-Start}$=+0.19 ‰, calculated using Eq. (1)). As an Si accumulator, wheat incorporated almost all available Si within six weeks. The remaining Si is strongly enriched in ^{30}Si ($^{Wheat}\Delta^{30}Si_{Solution:End-Start}$=+0.83 ‰). In week six one growth solution was so strongly depleted in Si that Si isotope ratios could not be determined.

Tomato plants incorporate light Si, where the bulk plant Si isotope composition, expressed as $^{Tomato}\Delta^{30}Si_{plants}$ averaged -0.27 ±0.06 ‰ ($^{Species}\Delta^{30}Si_{parts}$ are relative to the nutrient solution at the beginning, calculated using Eq. (2), and uncertainties are 95% CI). The Si present in the roots is isotopically indistinguishable from the nutrient solution ($^{Tomato}\Delta^{30}Si_{roots}$ = 0.01 ± 0.16 ‰), whereas the tomato shoots contain lighter Si ($^{Tomato}\Delta^{30}Si_{shoots}$ = -0.36 ±0.12 ‰). In contrast, mustard roots are lighter in their Si isotope composition ($^{Mustard}\Delta^{30}Si_{roots}$ = -0.77 ± 0.15 ‰) than the above-ground parts ($^{Mustard}\Delta^{30}Si_{shoots}$ = -0.05 ± 0.11 ‰). Nevertheless, mustard plants incorporated overall light Si ($^{Mustard}\Delta^{30}Si_{plants}$ = -0.45 ± 0.09 ‰). Since wheat consumed almost all available Si no significant fractionation between the plant and solution was observable ($^{Wheat}\Delta^{30}Si_{plants}$ = -0.07 ± 0.26 ‰). Most of the Si was deposited in the shoots, with an isotopic composition close to the composition of the starting solution ($^{Wheat}\Delta^{30}Si_{shoots}$ = -0.06 ± 0.26 ‰). The roots, however, preferentially stored light Si ($^{Wheat}\Delta^{30}Si_{roots}$ = -1.04 ± 0.34 ‰), similar to the mustard roots.

Our experimental setup allows us to determine the Si isotope fractionation factors into bulk plants directly from the temporal evolution of the Si isotope composition of the nutrient solution. This approach differs from previous studies of Si isotope fractionation by plants, in which the Si pool in the nutrient solution was frequently replenished (Ding et al., 2008a; Sun et al., 2008, 2016b). Evaluating the temporal evolution of wheat nutrient solution (Figure 3) and assuming no back-diffusion, a Rayleigh like fractionation can be fitted using Eq. (5) (Mariotti et al., 1981):

$$\frac{R}{R_0} = f_{solution}^{\alpha-1} \quad (5)$$

where $f_{solution}$ is the fraction of Si in the remaining solution, R_0 the initial $^{30}Si/^{28}Si$ isotope ratio, R the $^{30}Si/^{28}Si$ isotope ratio of the product, and α the fractionation factor. A best fit to the data, minimising the root-mean-square-deviation, results in $\alpha_{Plant-solution}$ for tomato of 0.99970 (1000·ln(α) = -0.33 ‰), for mustard an $\alpha_{Plant-solution}$ of 0.99945 (1000·ln(α) = -0.55 ‰), and for wheat an $\alpha_{Plant-solution}$ of 0.99957 (1000·ln(α) = -0.43 ‰), respectively (Figure 3). We use a Monte Carlo approach to estimate uncertainty on $\alpha_{Plant-solution}$, by calculating $\alpha_{Plant-solution}$ on 500 permutations of the dataset in which values for $\delta^{30}Si$ and Si concentration were randomly drawn from a normal distribution with means and standard deviations provided by the measurement (Table 5). Within uncertainty, there is no significant difference in the bulk fractionation factor between active and rejective uptake species. The best fit through all results, across the three plant species from this study, results in a fractionation factor 1000·ln(α) of -0.41 ± 0.09 ‰ (1 s) at an initial Si concentration of 49.5 $\mu g \cdot g^{-1}$ (ca. 1.76 mM).

If we assume the uptake of Si to be governed by diffusion through cell membranes and Si permeable transporters (Ma et al., 2006, 2007; Ma and Yamaji, 2015; Mitani et al., 2009; Zangi and Filella, 2012) and the diffusion of Si is non-quantitative, the

https://doi.org/10.5194/bg-2020-66
Preprint. Discussion started: 9 April 2020

lighter isotopes will be enriched in the target compartment (Sun et al., 2008; Weiss et al., 2004). To a first approximation, the difference between the diffusion coefficient of isotopologues $^{28}Si(OH)_4$ and $^{30}Si(OH)_4$ sets the theoretical upper limit of observable isotopic fractionation in a system dominated by diffusion. The diffusion coefficient ratio approximated by Eq. (6) corresponds to the fractionation factor in an idealised system consisting of pure water and silicic acid only (Mills and Harris, 1976; Richter et al., 2006).

$$\frac{D_{^{28}Si(OH)_4}}{D_{^{30}Si(OH)_4}} = \sqrt{\frac{\left(\frac{m_{^{30}Si(OH)_4} \times m_{H_2O}}{m_{^{30}Si(OH)_4} + m_{H_2O}}\right)}{\left(\frac{m_{^{28}Si(OH)_4} \times m_{H_2O}}{m_{^{28}Si(OH)_4} + m_{H_2O}}\right)}} \quad (6)$$

where D is the diffusion coefficient of a given Si molecule, and $m_{H_2O}, m_{^{28}Si(OH)_4}, m_{^{30}Si(OH)_4}$ are the molecular masses of the solvent (assuming pure water), $^{28}Si(OH)_4$ and $^{30}Si(OH)_4$, respectively. For $^{28}Si(OH)_4$ and $^{30}Si(OH)_4$ in pure water this results in a ratio of 0.99839 ($1000 \cdot \ln(\alpha)$ = -1.61 ‰). The observed α_{Plant} is about four times smaller (in $1000 \cdot \ln(\alpha)$ space) than the ideal diffusion coefficient ratio (-0.41 ‰ versus -1.61 ‰). The overestimation of the theoretical diffusion coefficient to the measured coefficient has been observed in other systems before (e.g. O'Leary, 1984).

4 Discussion

4.1 Reliability of the combined element and isotope ratio approach

In contrast to previous studies, we added a finite nutrient amount to growth solutions and replenished only the transpired water. The combination of plant physiological ratios (water use efficiency, element budgets and biomass production) with stable isotope ratio measurements allows us to explore the temporal evolution of Si uptake and translocation. Several aspects of our data attest to the reliability of our approach and results. Concerning Si uptake dynamics, Si recovery rates of >80% (see Table 3) corroborate the reliability of our results. The same is observed for the isotope budgets. There is no significant difference between the isotopic composition of the starting solution and the weighted average of the isotopic compositions of the different compartments at the end (see Table 4). This implies all significant pathways that fractionate Si isotopes have been accounted for. The Si retrieval rate between 83 and 90% is likely not caused by a single systematic analytical uncertainty or unaccounted sink of Si, but rather a combination of container wall absorption (up to 0.1%), root washing procedure (up to 1%), the weekly sampling (up to 3.5%) and analytical uncertainties (up to 10%). Guttation (Yamaji et al., 2008) and litter fall were not observed during the experiment.

4.2 Si uptake strategies

The ratio between measured Si uptake and the theoretical Si amount that would have entered the plant in a purely passive uptake mechanism (see section plant performance ratios), shows that wheat accumulates Si and mustard and tomato both reject Si (Figure 1 and Table 2). The accumulation of Si in wheat can be explained by the cooperation of an influx transporter (Lsi1-

https://doi.org/10.5194/bg-2020-66
Preprint. Discussion started: 9 April 2020

like) into the roots and the presumed presence of an efflux transporter (Lsi2-like) from the roots into the xylem. Closely related cereals have such transporters, therefore we expect them to be present in wheat too (Ma and Yamaji, 2015). In rice, mutants with either defective Lsi1 or Lsi2 transporter lead to significantly lower Si accumulation (Köster et al., 2009). The direct comparison between both mutants revealed that Lsi1 carries a larger share of Si incorporation, thus a defective Lsi2 can partially be compensated (Köster et al., 2009).

Our experiments show a striking similarity in Si uptake characteristics between mustard and tomato. Considering the differences in ontogenesis between the plant species, this may be a fortuitous coincidence. In particular, the relatively low temperatures may have inhibited the growth of the more thermophilic tomato, while the conditions were closer to optimal for mustard and summer wheat. Tomatoes have the genetic capacity to accumulate Si, since an orthologue of Lsi1 is present in the genes. An insertion in the amino acid sequence however, lead to a loss of the Si uptake functionality (Deshmukh et al., 2016, 2015), and thus tomato like mustard, rejects Si.

With our experimental approach we also detect significant differences between the crop species in Si transfer from the root to the shoot (Table 2). Wheat, which probably has a metabolically active efflux transporter (Lsi2-like) at the root-xylem interface, has the highest Si transfer efficiency per water mass (49.3 ± 8.4 mg shoot $Si \cdot L^{-1}$). The transfer efficiency for tomato is significantly higher than mustard (3.5 ± 0.4, and 2.4 ± 0.3 mg shoot $Si \cdot L^{-1}$, respectively), which is not readily explainable by differences in root Si efflux pathways since tomato does not contain the active efflux transporter orthologue Lsi2 while mustard does (Ma & Yamaji, 2015; Sonah *et al.*, 2017). Phytolith formation, which was observed in mustard roots (data not shown) could explain the lower Si transfer efficiency of mustard. A similar immobilization of silica in roots has already been observed in wheat (Hodson and Sangster, 1989) and other grasses (Paolicchi et al., 2019). Other possible reasons for this phenomenon will be discussed based on the results on Si isotope fractionation.

4.3 Dynamics of Si isotope fractionation during uptake

The plant performance parameters show that there are two distinctly different Si uptake mechanisms present: an active strategy in wheat, and a rejective strategy in tomato and mustard. Despite these different Si uptake mechanisms, we find preferential uptake of light Si isotopes observed in all three species with the average $1000 \cdot \ln(\alpha)$ of -0.41 ± 0.09 ‰ (1 s). We can only speculate on the reasons for the plants' preference for ^{28}Si over ^{30}Si. Si is taken up (actively facilitated) through Si permeable channels (orthologues of Lsi1 in rice, maize and barley) and passively with the water flow. Nowhere along these pathways does a change in the coordination sphere of silicic acid occur (Ma et al., 2006, 2007; Mitani et al., 2009) which could lead to the preferential incorporation of the heavy Si isotope in the fraction taken up. Thus we speculate that both pathways favour the light isotopologue because of its greater diffusion coefficient (Sun et al., 2008; Weiss et al., 2004), a process for which a predicted maximum isotope fractionation of -1.6‰ (based on Eq. (6)) is expected. While the processes of active and rejective Si uptake differ in the amounts of Si (per time, and root mass) taken up into the plants, we speculate that the physico-chemical

https://doi.org/10.5194/bg-2020-66
Preprint. Discussion started: 9 April 2020

processes governing Si uptake, which induce the stable isotope fractionation, are identical at a given initial concentration in the nutrient solution.

Our new Si fractionation factors are similar to those measured in other species, including rice, -0.30 ‰ (Sun et al., 2008), -0.53 ± 0.17 ‰ (for $^{29/28}$Si, recalculated to $^{30/28}$Si: -1.02 ± 0.33 ‰, Ding et al., 2005) and -0.79 ± 0.07 (Sun et al., 2016a), banana, -0.40 ± 0.11 ‰ (for $^{29/28}$Si, recalculated to $^{30/28}$Si: -0.77 ± 0.21 ‰, Opfergelt et al., 2006) and -0.35 ‰ (for $^{29/28}$Si, recalculated to $^{30/28}$Si: -0.68 ‰, Delvigne et al., 2009), and corn and wheat, -0.52± 0.16 ‰ (for $^{29/28}$Si, recalculated to $^{30/28}$Si: -1.00 ± 0.31 ‰, Ziegler et al., 2005). The only positive fractionations for Si isotopes reported are by Y. Sun and co-workers (Sun et al., 2016b) for rice (+0.38 and -0.32 ‰) and cucumber (+0.27 and +0.20 ‰). Previous experiments with the same rice species by L. Sun *et al.* however yielded a fractionation factor of -0.30 ‰ (Sun et al., 2008). These authors speculate that an active uptake mechanism preferentially incorporates heavy Si isotopes – a hypothesis that is not supported by our results.

4.4 Silicon fractionation between the roots and shoots

The presence or absence of the efflux (Lsi2-like metabolically active) transporter allows to explore its influence on isotope fractionation in the root and during further transport. (1) If Lsi2 has a similar functionality as Lsi1, a preference for the light ^{28}Si as caused by diffusion should emerge which would be indistinguishable from the passive diffusion in the absence of Lsi2. (2) Alternatively, the presence of Lsi2 could also induce equilibrium isotope fractionation during a change in the speciation of silicic acid, causing the preferential transport of either ^{28}Si or ^{30}Si. (3) The third possibility are indirect effects in the roots such as precipitation of silicic acid in the roots which enrich the remaining silicic acid which is transported into the shoots in heavy ^{30}Si.

The three crop species show large differences in their root Si isotopic composition. Mustard and spring wheat preferentially store light ^{28}Si in their roots ($^{Mustard}\Delta^{30}Si_{roots}$ -0.77 ± 0.15 ‰, $^{Wheat}\Delta^{30}Si_{roots}$ -1.04 ± 0.34 ‰, relative to the nutrient solution) whereas tomato does not show a preference for either the lighter or heavier silicon isotopes ($^{Tomato}\Delta^{30}Si_{roots}$ -0.01 ± 0.16 ‰). The further transport of Si from the roots into the xylem seems not be driven by a diffusion process through Lsi2. Thus, hypothesis (1), that Lsi2 has a similar functionality as Lsi1 and transports Si in a diffusive process, is not applicable. For mustard and wheat orthologues of Lsi2 have been shown to be involved in the Si transport (Deshmukh et al., 2016; Sonah et al., 2017). The current understanding of the molecular functionality of Lsi2 however, provides not enough evidence for an equilibrium process where a preferential transport of ^{30}Si over ^{28}Si into the xylem would be expected (hypothesis 2).

The isotopic difference between the Si in the shoots and in the roots ($^{30}\Delta_{Root\text{-}Shoot}$) for mustard and wheat, amounts to -0.72 and -0.98 ‰, respectively, and could be explained by precipitation reactions in the roots (for wheat mineral depositions in the roots have been observed see Hodson & Sangster, 1989, supporting hypothesis 3). Precipitation of biogenic silica would enrich the mobile silicon pool in the root in heavy ^{30}Si, which is then transported into the shoots. Köster *et al.*, 2009, showed that rice mutants with a defective Lsi2 lead to an additional (compared to non-mutants) preferential transport of heavy ^{30}Si into the

https://doi.org/10.5194/bg-2020-66
Preprint. Discussion started: 9 April 2020

straw. This could be explained by an oversaturation in the roots due to the missing efflux transporter (Lsi2), leading to additional biogenic silica precipitation in the roots. The positive $^{30}\Delta_{Root\text{-}Shoot}$ of +0.37 ‰ for tomato, where Lsi2 is absent, indicate that the pool of Si in the roots was depleted in ^{28}Si by a preferential diffusion process of the lighter isotope.

4.5 Implications for terrestrial Si isotope cycling

Several field based studies have investigated the isotope fractionation induced by plants (Cornelis et al., 2011; Ding et al., 2005; Frings et al., 2014; Opfergelt et al., 2010; White et al., 2012) In contrast to field based studies, the stable silicon isotope fractionation determined on bulk plants show a very narrow range from -1.02 to -0.30 ‰ with the exception of the positive fractionation factors by Sun et al., 2016b. The determined Si isotope fractionation factors in laboratory experiments indicate that the physico-chemical processes governing Si uptake in a wide range of different plant species, are identical under a broad range of laboratory (environmental) conditions. The broader and larger magnitude of isotope fractionation observed in natural settings could be an observational bias when analysing and extrapolating from individual plant parts to whole plant fractionation and the challenges associated with characterisation of the plant available silicon pool. Our results demonstrate that the fractionation between roots and shoots is variable in direction and is controlled by internal plant processes, which are likely also being present within subparts of the roots and shoots.

This implies that Si which is liberated through weathering reactions, may be recycled multiple times through plants, re-dissolved into soil solution and precipitated into secondary minerals before being exported from the ecosystem as biogenic silica, secondary clays, or as dissolved Si. The relative magnitude between these fluxes depends however on the environmental conditions (Frings et al., 2016; Sommer et al., 2006, 2013). The isotope composition of the dissolved Si in river water shows almost exclusively a heavier silicon isotope signature than the bedrock they drain (Frings et al., 2016; Opfergelt and Delmelle, 2012). To close the Si isotopic mass balance therefore requires an isotopically light solid counterpart (Bouchez et al., 2013). The plant and phytolith data aggregated by Frings et al., 2016 suggest that biogenic silica is unlikely one of the main export flux of Si from catchments. Plants are an important factor for the internal ecosystem element cycling (Uhlig and von Blanckenburg, 2019), but not for the particulate Si export.

5 Conclusion

We have confirmed that Si uptake into crop plants is species-specific and complex, involving rejective, passive and active processes in varying proportions. Regardless of the uptake strategy (active and rejective) all three crop species preferentially incorporate light silicon (^{28}Si) with a fractionation factor $1000 \cdot \ln(\alpha)$ for tomato -0.33 ‰, for mustard -0.55 ‰ and for wheat -0.43 ‰. Within uncertainty, the fractionation factors between these species are indistinguishable. This similarity indicates that the physico-chemical processes governing Si uptake, whether active or passive, or with Lsi1-like transporters present or absent, are identical. The incorporation and fractionation of stable Si isotope ratios at the root epidermis is likely

https://doi.org/10.5194/bg-2020-66
Preprint. Discussion started: 9 April 2020

400 governed by the preferential diffusion of the lighter homologue of silicic acid. In contrast at the root endodermis, for species with the Lsi2-like transporter (wheat and mustard), the further transport of silicic acid from the roots into the xylem and shoots is not controlled by the preferential diffusion of light ^{28}Si. A likely change in the chemical environment in the roots results in the precipitation of biogenic silica, which is enriched in ^{28}Si over ^{30}Si. The remaining silicic acid which is transported and deposited in the shoots is thus enriched in ^{30}Si. For plant species where the biogenic silica precipitation is absent, the transport
405 is governed by a diffusion process and hence preferentially light silicon ^{28}Si is transported into the shoots. A full description of the isotope and elemental fractionation during transport of silicic acid and precipitation of biogenic silica requires a better understanding of the biological processes and molecules involved in the dehydration of silicic acid to amorphous silica (He et al., 2015; Leng et al., 2009). Here, the toolbox of isotope geochemistry is well-poised, e.g. temporal isotope-spiking experiments during a short period of the plant growth and ripening can deliver insights into the mobility and pathways of newly
410 and formerly acquired silicic acid.

Author Contribution

All authors designed the study, D. A. F. and R. R. have grown the plants, D. A. F. has analysed the samples and evaluated the data, prepared the figures. All authors have contributed to the discussion, interpretation and writing of this manuscript.

Competing interests

415 The authors declare that they have no conflict of interest.

Acknowledgments

D.A.F. thanks the Swiss National Science Foundation for an Early Postdoc.Mobility fellowship (P2EZP2_168836), the GFZ German Research Centre for Geosciences, Helmholtz Laboratory for the Geochemistry of the Earth Surface (HELGES) and the Leibniz Centre for Agricultural Landscape Research for providing excellent (laboratory) infrastructure. The authors would
420 like to thank Christian Buhtz for taking care of the plants during the hydroponic experiments. D.A.F. would like to thank Josefine Buhk and Jutta Schlegel for their support in HELGES.

Data availability

All data used in this study are available in the supplementary, containing the tables S1– S4.

https://doi.org/10.5194/bg-2020-66
Preprint. Discussion started: 9 April 2020

References

425 Blanck, E., Melville, R. and Sachse, J.: Zur Bestimmung des Gesamtschwefelgehaltes in der Pflanzensubstanz, Bodenkd. und Pflanzenernährung, 6(1–2), 56–64, doi:10.1002/jpln.19380060106, 1938.

Blecker, S. W., King, S. L., Derry, L. A., Chadwick, O. A., Ippolito, J. A. and Kelly, E. F.: The ratio of germanium to silicon in plant phytoliths: Quantification of biological discrimination under controlled experimental conditions, Biogeochemistry, 86(2), 189–199, doi:10.1007/s10533-007-9154-7, 2007.

430 Bouchez, J., von Blanckenburg, F. and Schuessler, J. A.: Modeling novel stable isotope ratios in the weathering zone, Am. J. Sci., 313(4), 267–308, doi:10.2475/04.2013.01, 2013.

Broadley, M., Brown, P., Cakmak, I., Ma, J. F., Rengel, Z. and Zhao, F.: Beneficial Elements, in Marschner's Mineral Nutrition of Higher Plants, pp. 249–269, Elsevier., 2012.

Carey, J. C. and Fulweiler, R. W.: The Terrestrial Silica Pump, PLoS One, 7(12), doi:10.1371/journal.pone.0052932, 2012.

435 Coplen, T. B., Hopple, J. a, Böhlke, J. K., Peiser, H. S., Rieder, S. E., Krouse, H. R., Rosman, K. J. R., Ding, T., Vocke, R. D. J., Révész, K. M., Lamberty, A., Taylor, P. and Bièvre, P. De: Compilation of minimum and maximum isotope ratios of selected elements in naturally occurring terrestrial materials and reagents, U.S. Geol. Surv. Water-Resources Investig. Rep. 01-4222, 45–50 [online] Available from: http://pubs.usgs.gov/wri/wri014222/, 2002.

Cornelis, J.-T., Delvaux, B., Georg, R. B., Lucas, Y., Ranger, J. and Opfergelt, S.: Tracing the origin of dissolved silicon
440 transferred from various soil-plant systems towards rivers: a review, Biogeosciences, 8(1), 89–112, doi:10.5194/bg-8-89-2011, 2011.

Cornelis, J.-T. T., Delvaux, B., Cardinal, D., André, L., Ranger, J. and Opfergelt, S.: Tracing mechanisms controlling the release of dissolved silicon in forest soil solutions using Si isotopes and Ge/Si ratios, Geochim. Cosmochim. Acta, 74(14), 3913–3924, doi:10.1016/j.gca.2010.04.056, 2010.

445 Coskun, D., Deshmukh, R., Sonah, H., Menzies, J. G., Reynolds, O., Ma, J. F., Kronzucker, H. J. and Bélanger, R. R.: The controversies of silicon's role in plant biology, New Phytol., nph.15764, doi:10.1111/nph.15343, 2019.

Delvigne, C., Opfergelt, S., Cardinal, D., Delvaux, B. and André, L.: Distinct silicon and germanium pathways in the soil-plant system: Evidence from banana and horsetail, J. Geophys. Res. Biogeosciences, 114(G2), n/a-n/a, doi:10.1029/2008JG000899, 2009.

450 Derry, L. A., Kurtz, A. C., Ziegler, K. and Chadwick, O. A.: Biological control of terrestrial silica cycling and export fluxes to watersheds., Nature, 433(7027), 728–731, doi:10.1038/nature03299, 2005.

Deshmukh, R., Bélanger, R. R. and Hartley, S.: Molecular evolution of aquaporins and silicon influx in plants, Funct. Ecol., 30(8), 1277–1285, doi:10.1111/1365-2435.12570, 2016.

Deshmukh, R. K., Vivancos, J., Ramakrishnan, G., Guérin, V., Carpentier, G., Sonah, H., Labbé, C., Isenring, P., Belzile, F.
455 J. and Bélanger, R. R.: A precise spacing between the NPA domains of aquaporins is essential for silicon permeability in plants, Plant J., 83(3), 489–500, doi:10.1111/tpj.12904, 2015.

https://doi.org/10.5194/bg-2020-66
Preprint. Discussion started: 9 April 2020

Ding, T. P., Ma, G. R., Shui, M. X., Wan, D. F. and Li, R. H.: Silicon isotope study on rice plants from the Zhejiang province, China, Chem. Geol., 218(1-2 SPEC. ISS.), 41–50, doi:10.1016/j.chemgeo.2005.01.018, 2005.

Ding, T. P., Tian, S. H., Sun, L., Wu, L. H., Zhou, J. X. and Chen, Z. Y.: Silicon isotope fractionation between rice plants and nutrient solution and its significance to the study of the silicon cycle, Geochim. Cosmochim. Acta, 72(23), 5600–5615, doi:10.1016/j.gca.2008.09.006, 2008a.

Ding, T. P., Zhou, J. X., Wan, D. F., Chen, Z. Y., Wang, C. Y. and Zhang, F.: Silicon isotope fractionation in bamboo and its significance to the biogeochemical cycle of silicon, Geochim. Cosmochim. Acta, 72(5), 1381–1395, doi:10.1016/j.gca.2008.01.008, 2008b.

Epstein, E.: The anomaly of silicon in plant biology., Proc. Natl. Acad. Sci. U. S. A., 91(1), 11–17, doi:10.1073/pnas.91.1.11, 1994.

Epstein, E.: Silicon, Annu. Rev.Plant Physiol. Plant Mol. Biol., (50), 641–664, 1999.

Epstein, E.: Chapter 1 Silicon in plants: Facts vs. concepts, in Studies in Plant Science, vol. 8, pp. 1–15., 2001.

Exley, C. and Guerriero, G.: A reappraisal of biological silicification in plants?, New Phytol., nph.15764, doi:10.1111/nph.15752, 2019.

Frings, P. J., De La Rocha, C., Struyf, E., van Pelt, D., Schoelynck, J., Hudson, M. M., Gondwe, M. J., Wolski, P., Mosimane, K., Gray, W., Schaller, J. and Conley, D. J.: Tracing silicon cycling in the Okavango Delta, a sub-tropical flood-pulse wetland using silicon isotopes, Geochim. Cosmochim. Acta, 142, 132–148, doi:10.1016/j.gca.2014.07.007, 2014.

Frings, P. J., Clymans, W., Fontorbe, G., De La Rocha, C. L. and Conley, D. J.: The continental Si cycle and its impact on the ocean Si isotope budget, Chem. Geol., 425, 12–36, doi:10.1016/j.chemgeo.2016.01.020, 2016.

Geilert, S., Vroon, P. Z., Roerdink, D. L., Van Cappellen, P. and van Bergen, M. J.: Silicon isotope fractionation during abiotic silica precipitation at low temperatures: Inferences from flow-through experiments, Geochim. Cosmochim. Acta, 142(1), 95–114, doi:10.1016/j.gca.2014.07.003, 2014.

Georg, R. B., Reynolds, B. C., Frank, M. and Halliday, A. N.: New sample preparation techniques for the determination of Si isotopic compositions using MC-ICPMS, Chem. Geol., 235(1–2), 95–104, doi:10.1016/j.chemgeo.2006.06.006, 2006.

He, C., Ma, J. and Wang, L.: A hemicellulose-bound form of silicon with potential to improve the mechanical properties and regeneration of the cell wall of rice, New Phytol., 206(3), 1051–1062, doi:10.1111/nph.13282, 2015.

He, H. tao, Zhang, S., Zhu, C. and Liu, Y.: Equilibrium and kinetic Si isotope fractionation factors and their implications for Si isotope distributions in the Earth's surface environments, Acta Geochim., 35(1), 15–24, doi:10.1007/s11631-015-0079-x, 2016.

Hodson, M. J. and Sangster, A. G.: Subcellular localization of mineral deposits in the roots of wheat (Triticum aestivum L.), Protoplasma, 151(1), 19–32, doi:10.1007/BF01403298, 1989.

Hodson, M. J., White, P. J., Mead, A. and Broadley, M. R.: Phylogenetic variation in the silicon composition of plants, Ann. Bot., 96(6), 1027–1046, doi:10.1093/aob/mci255, 2005.

Köster, J. R., Bol, R., Leng, M. J., Parker, A. G., Sloane, H. J. and Ma, J. F.: Effects of active silicon uptake by rice on 29Si

fractionation in various plant parts, Rapid Commun. Mass Spectrom., 23(16), 2398–2402, doi:10.1002/rcm.3971, 2009.

Leng, M. J., Swann, G. E. A., Hodson, M. J., Tyler, J. J., Patwardhan, S. V. and Sloane, H. J.: The Potential use of Silicon Isotope Composition of Biogenic Silica as a Proxy for Environmental Change, Silicon, 1(2), 65–77, doi:10.1007/s12633-009-9014-2, 2009.

Ma, J. F.: Role of silicon in enhancing the resistance of plants to biotic and abiotic stresses, Soil Sci. Plant Nutr., 50(1), 11–18, doi:10.1080/00380768.2004.10408447, 2004.

Ma, J. F. and Yamaji, N.: Silicon uptake and accumulation in higher plants, Trends Plant Sci., 11(8), 392–397, doi:10.1016/j.tplants.2006.06.007, 2006.

Ma, J. F. and Yamaji, N.: A cooperative system of silicon transport in plants, Trends Plant Sci., 20(7), 435–442, doi:10.1016/j.tplants.2015.04.007, 2015.

Ma, J. F., Miyake, Y. and Takahashi, E.: Chapter 2 Silicon as a beneficial element for crop plants, in Studies in Plant Science, vol. 8, pp. 17–39., 2001.

Ma, J. F., Tamai, K., Yamaji, N., Mitani, N., Konishi, S., Katsuhara, M., Ishiguro, M., Murata, Y. and Yano, M.: A silicon transporter in rice, Nature, 440(7084), 688–691, doi:10.1038/nature04590, 2006.

Ma, J. F., Yamaji, N., Mitani, N., Tamai, K., Konishi, S., Fujiwara, T., Katsuhara, M. and Yano, M.: An efflux transporter of silicon in rice, Nature, 448(7150), 209–212, doi:10.1038/nature05964, 2007.

Mariotti, A., Germon, J. C., Hubert, P., Kaiser, P., Letolle, R., Tardieux, A. and Tardieux, P.: Experimental determination of nitrogen kinetic isotope fractionation: Some principles; illustration for the denitrification and nitrification processes, Plant Soil, 62(3), 413–430, doi:10.1007/BF02374138, 1981.

Marron, A. O., Chappell, H., Ratcliffe, S. and Goldstein, R. E.: A model for the effects of germanium on silica biomineralization in choanoflagellates, J. R. Soc. Interface, 13(122), doi:10.1098/rsif.2016.0485, 2016.

Marschner, H. and Marschner, P.: Marschner's mineral nutrition of higher plants, Academic Press. [online] Available from: https://www.sciencedirect.com/science/book/9780123849052 (Accessed 5 April 2018), 2012.

Mills, R. and Harris, K. R.: The effect of isotopic substitution on diffusion in liquids, Chem. Soc. Rev., 5, 215, doi:10.1039/cs9760500215, 1976.

Mitani, N., Chiba, Y., Yamaji, N. and Ma, J. F.: Identification and Characterization of Maize and Barley Lsi2-Like Silicon Efflux Transporters Reveals a Distinct Silicon Uptake System from That in Rice, Plant Cell, 21(7), 2133–2142, doi:10.1105/tpc.109.067884, 2009.

Mühling, K. H. and Sattelmacher, B.: Apoplastic Ion Concentration of Intact Leaves of Field Bean (Vicia faba) as Influenced by Ammonium and Nitrate Nutrition, J. Plant Physiol., 147(1), 81–86, doi:10.1016/S0176-1617(11)81417-3, 1995.

O'Leary, M. H.: Measurement of the isotope fractionation associated with diffusion of carbon dioxide in aqueous solution, J. Phys. Chem., 88(4), 823–825, doi:10.1021/j150648a041, 1984.

Oelze, M., von Blanckenburg, F., Bouchez, J., Hoellen, D. and Dietzel, M.: The effect of Al on Si isotope fractionation investigated by silica precipitation experiments, Chem. Geol., 397, 94–105, doi:10.1016/j.chemgeo.2015.01.002, 2015.

525 Oelze, M., Schuessler, J. A. and von Blanckenburg, F.: Mass bias stabilization by Mg doping for Si stable isotope analysis by MC-ICP-MS, J. Anal. At. Spectrom., 31(10), 2094–2100, doi:10.1039/C6JA00218H, 2016.

Opfergelt, S. and Delmelle, P.: Silicon isotopes and continental weathering processes: Assessing controls on Si transfer to the ocean, Comptes Rendus - Geosci., 344(11–12), 723–738, doi:10.1016/j.crte.2012.09.006, 2012.

Opfergelt, S., Cardinal, D., Henriet, C., Draye, X., André, L. and Delvaux, B.: Silicon Isotopic Fractionation by Banana (Musa
530 spp.) Grown in a Continuous Nutrient Flow Device, Plant Soil, 285(1–2), 333–345, doi:10.1007/s11104-006-9019-1, 2006.

Opfergelt, S., Cardinal, D., André, L., Delvigne, C., Bremond, L. and Delvaux, B.: Variations of δ30Si and Ge/Si with weathering and biogenic input in tropical basaltic ash soils under monoculture, Geochim. Cosmochim. Acta, 74(1), 225–240, doi:10.1016/j.gca.2009.09.025, 2010.

Paolicchi, M., Benvenuto, M. L., Honaine, M. F. and Osterrieth, M.: Root silicification of grasses and crops from the Pampean
535 region and its relevance to silica and silicophytolith content of soils, Plant Soil, doi:10.1007/s11104-019-04287-4, 2019.

Poitrasson, F.: Silicon Isotope Geochemistry, Rev. Mineral. Geochemistry, 82, 289–344, doi:10.2138/rmg.2017.82.8, 2017.

Pokrovski, G. S. and Schott, J.: Experimental study of the complexation of silicon and germanium with aqueous organic species: Implications for germanium and silicon transport and Ge/Si ratio in natural waters, Geochim. Cosmochim. Acta, 62(21–22), 3413–3428, 1998.

540 Raven, J. A.: Chapter 3 Silicon transport at the cell and tissue level, in Studies in Plant Science, vol. 8, pp. 41–55., 2001.

Richmond, K. E. and Sussman, M.: Got silicon? The non-essential beneficial plant nutrient, Curr. Opin. Plant Biol., 6(3), 268–272, doi:10.1016/S1369-5266(03)00041-4, 2003.

Richter, F. M., Mendybaev, R. A., Christensen, J. N., Hutcheon, I. D., Williams, R. W., Sturchio, N. C. and Beloso, A. D.: Kinetic isotopic fractionation during diffusion of ionic species in water, Geochim. Cosmochim. Acta, 70(2), 277–289,
545 doi:10.1016/j.gca.2005.09.016, 2006.

Roerdink, D. L., van den Boorn, S. H. J. M., Geilert, S., Vroon, P. Z. and van Bergen, M. J.: Experimental constraints on kinetic and equilibrium silicon isotope fractionation during the formation of non-biogenic chert deposits, Chem. Geol., 402, 40–51, doi:10.1016/j.chemgeo.2015.02.038, 2015.

Schilling, G., Ansorge, H., Borchmann, W., Markgraf, G. and Peschke, H.: Pflanzenernährung und Düngung, VEB Deutscher
550 Landwirtschaftsverlag., 1982.

Schuessler, J. A. and von Blanckenburg, F.: Testing the limits of micro-scale analyses of Si stable isotopes by femtosecond laser ablation multicollector inductively coupled plasma mass spectrometry with application to rock weathering, Spectrochim. Acta Part B At. Spectrosc., 98, 1–18, doi:10.1016/j.sab.2014.05.002, 2014.

Schuessler, J. A., Kämpf, H., Koch, U. and Alawi, M.: Earthquake impact on iron isotope signatures recorded in mineral spring
555 water, J. Geophys. Res. Solid Earth, 121(12), 8548–8568, doi:10.1002/2016JB013408, 2016.

Sommer, M., Kaczorek, D., Kuzyakov, Y. and Breuer, J.: Silicon pools and fluxes in soils and landscapes—a review, J. Plant Nutr. Soil Sci., 169(3), 310–329, doi:10.1002/jpln.200521981, 2006.

Sommer, M., Jochheim, H., Höhn, A., Breuer, J., Zagorski, Z., Busse, J., Barkusky, D., Meier, K., Puppe, D., Wanner, M. and

https://doi.org/10.5194/bg-2020-66
Preprint. Discussion started: 9 April 2020

Kaczorek, D.: Si cycling in a forest biogeosystem - the importance of transient state biogenic Si pools, Biogeosciences, 10(7), 4991–5007, doi:10.5194/bg-10-4991-2013, 2013.

Sonah, H., Deshmukh, R. K., Labbé, C. and Bélanger, R. R.: Analysis of aquaporins in Brassicaceae species reveals high-level of conservation and dynamic role against biotic and abiotic stress in canola, Sci. Rep., 7(1), 1–17, doi:10.1038/s41598-017-02877-9, 2017.

Sparks, J. P., Chandra, S., Derry, L. A., Parthasarathy, M. V., Daugherty, C. S. and Griffin, R.: Subcellular localization of silicon and germanium in grass root and leaf tissues by SIMS: Evidence for differential and active transport, Biogeochemistry, 104(1–3), 237–249, doi:10.1007/s10533-010-9498-2, 2011.

Stamm, F. M., Zambardi, T., Chmeleff, J., Schott, J., von Blanckenburg, F. and Oelkers, E. H.: The experimental determination of equilibrium Si isotope fractionation factors among H4SiO4o, H3SiO4− and amorphous silica (SiO2·0.32 H2O) at 25 and 75 °C using the three-isotope method, Geochim. Cosmochim. Acta, 255, 49–68, doi:10.1016/j.gca.2019.03.035, 2019.

Sun, L., Wu, L. H., Ding, T. P. and Tian, S. H.: Silicon isotope fractionation in rice plants, an experimental study on rice growth under hydroponic conditions, Plant Soil, 304(1–2), 291–300, doi:10.1007/s11104-008-9552-1, 2008.

Sun, Y., Wu, L. and Li, X.: Experimental Determination of Silicon Isotope Fractionation in Rice, edited by H. Gerós, PLoS One, 11(12), e0168970, doi:10.1371/journal.pone.0168970, 2016a.

Sun, Y., Wu, L., Li, X., Sun, L., Gao, J. and Ding, T.: Silicon Isotope Fractionation in Rice and Cucumber Plants over a Life Cycle: Laboratory Studies at Different External Silicon Concentrations, J. Geophys. Res. Biogeosciences, 2829–2841, doi:10.1002/2016JG003443, 2016b.

Takahashi, E., Ma, J. F. and Miyake, Y.: The possibility of silicon as an essential element for higher plants, Comments Agric. Food Chem., 2(2), 99–102, 1990.

Uhlig, D. and von Blanckenburg, F.: How slow rock weathering balances nutrient loss during fast forest floor turnover in montane, temperate forest ecosystems, Front. Earth Sci., 7(July), doi:10.3389/feart.2019.00159, 2019.

Weiss, D. J., Mason, T. F. D., Zhao, F. J., Kirk, G. J. D., Coles, B. J. and Horstwood, M. S. A.: Isotopic discrimination of zinc in higher plants, New Phytol., 165(3), 703–710, doi:10.1111/j.1469-8137.2004.01307.x, 2004.

White, A. F., Vivit, D. V., Schulz, M. S., Bullen, T. D., Evett, R. R. and Aagarwal, J.: Biogenic and pedogenic controls on Si distributions and cycling in grasslands of the Santa Cruz soil chronosequence, California, Geochim. Cosmochim. Acta, 94, 72–94, doi:10.1016/j.gca.2012.06.009, 2012.

Wiche, O., Székely, B., Moschner, C. and Heilmeier, H.: Germanium in the soil-plant system—a review, Environ. Sci. Pollut. Res., 25(32), 31938–31956, doi:10.1007/s11356-018-3172-y, 2018.

Yamaji, N., Mitatni, N. and Ma, J. F.: A Transporter Regulating Silicon Distribution in Rice Shoots, Plant Cell, 20(5), 1381–1389, doi:10.1105/tpc.108.059311, 2008.

YAN, G., Nikolic, M., YE, M., XIAO, Z. and LIANG, Y.: Silicon acquisition and accumulation in plant and its significance for agriculture, J. Integr. Agric., 17(10), 2138–2150, doi:10.1016/S2095-3119(18)62037-4, 2018.

Zambardi, T. and Poitrasson, F.: Precise Determination of Silicon Isotopes in Silicate Rock Reference Materials by MC-ICP-

https://doi.org/10.5194/bg-2020-66
Preprint. Discussion started: 9 April 2020

MS, Geostand. Geoanalytical Res., 35(1), 89–99, doi:10.1111/j.1751-908X.2010.00067.x, 2011.

Zangi, R. and Filella, M.: Transport routes of metalloids into and out of the cell: A review of the current knowledge, Chem. Biol. Interact., 197(1), 47–57, doi:10.1016/j.cbi.2012.02.001, 2012.

Ziegler, K., Chadwick, O. A., Brzezinski, M. A. and Kelly, E. F.: Natural variations of δ30Si ratios during progressive basalt weathering, Hawaiian Islands, Geochim. Cosmochim. Acta, 69(19), 4597–4610, doi:10.1016/j.gca.2005.05.008, 2005.

https://doi.org/10.5194/bg-2020-66
Preprint. Discussion started: 9 April 2020

600 **Figures**

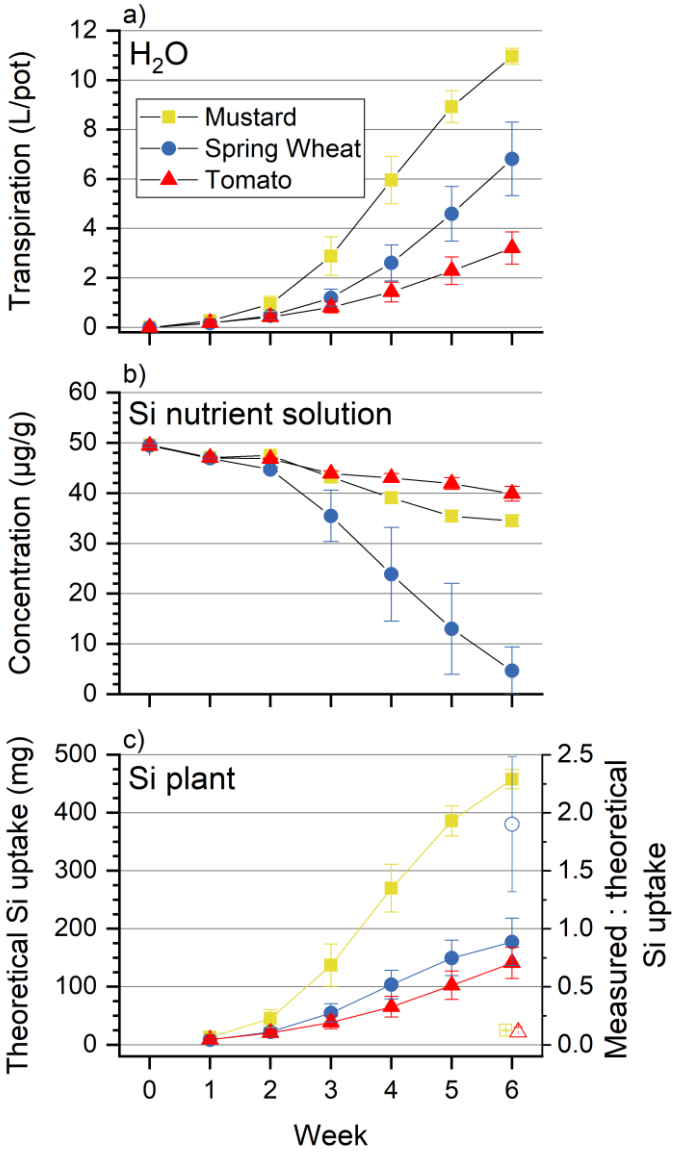

Figure 1: Cumulative transpiration (a), Si concentration in the nutrient solution (in µg/g, panel b) and the theoretical Si uptake through transpiration of tomato, mustard and spring wheat during 6 weeks (panel c). Mean ± standard deviation from 3 pots with 4 plants each. A ratio of measured and theoretical Si uptake (open symbols) of greater than 1 indicates an active uptake mechanism,
605 **a ratio much smaller than 1 a rejective strategy.**

https://doi.org/10.5194/bg-2020-66
Preprint. Discussion started: 9 April 2020

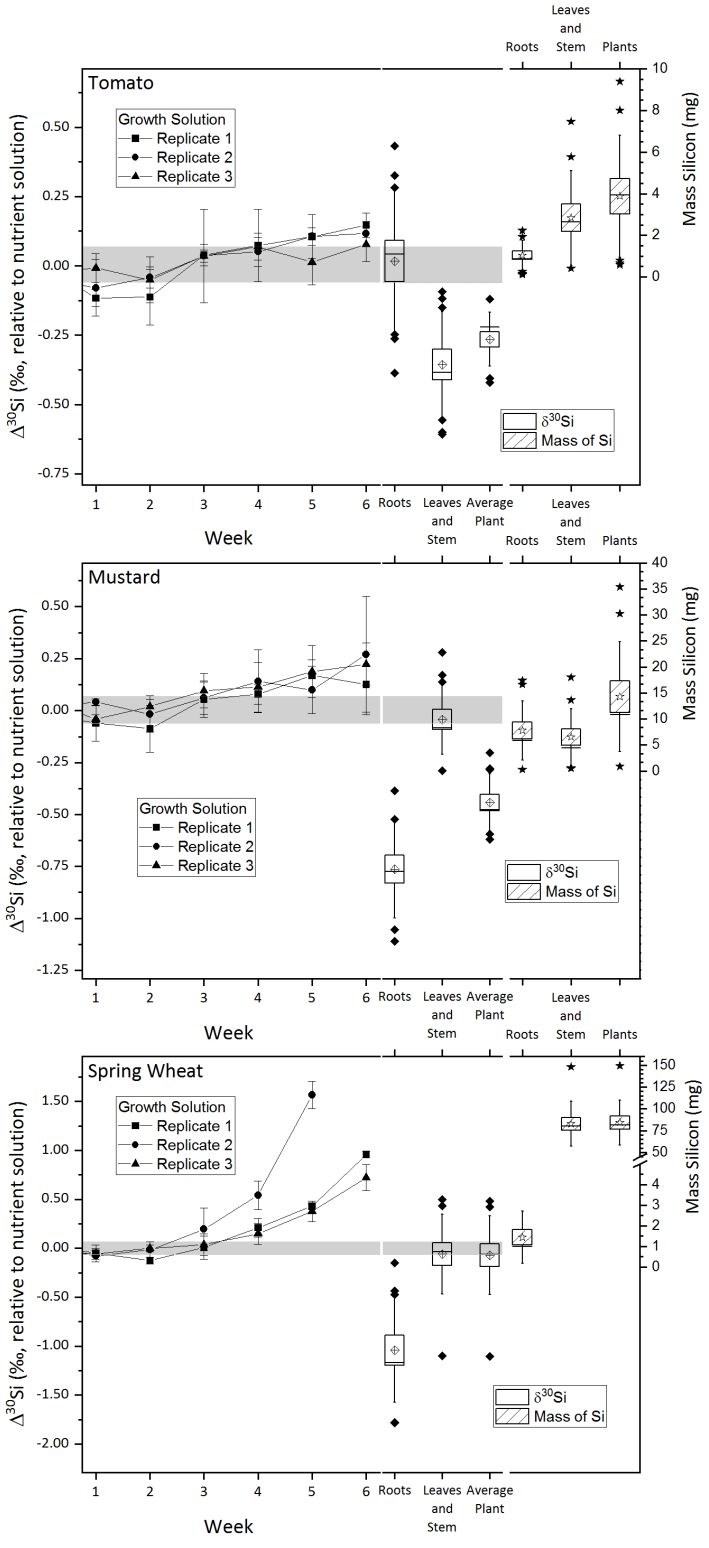

Figure 2: Silicon isotope composition during the growth of tomato (top panel), mustard (mid panel) and wheat (bottom panel). On the left y-axis the $\delta^{30}Si$ composition in ‰ relative to nutrient solution is reported, on the right y-axis the mass of silicon in mg incorporated by the plants. Uncertainty bars are based on 2 standard uncertainties, grey bar is the silicon isotopic composition of the starting solution ± two standard deviations. The box size is one standard uncertainty, whisker indicate one standard deviation, vertical line in the box is the median, empty diamond/stars in the box indicate the mean and filed diamonds/stars are outliers, outside of one standard deviation. Line plot is the weekly sampled nutrient solution (from week 1 to 6), the box plots are the plant samples, per species 12 roots and 12 leaves and stem samples were analysed, average were weighted by organ mass (calculated using Eq. (2)).

https://doi.org/10.5194/bg-2020-66
Preprint. Discussion started: 9 April 2020

Biogeosciences
Discussions
Open Access
EGU

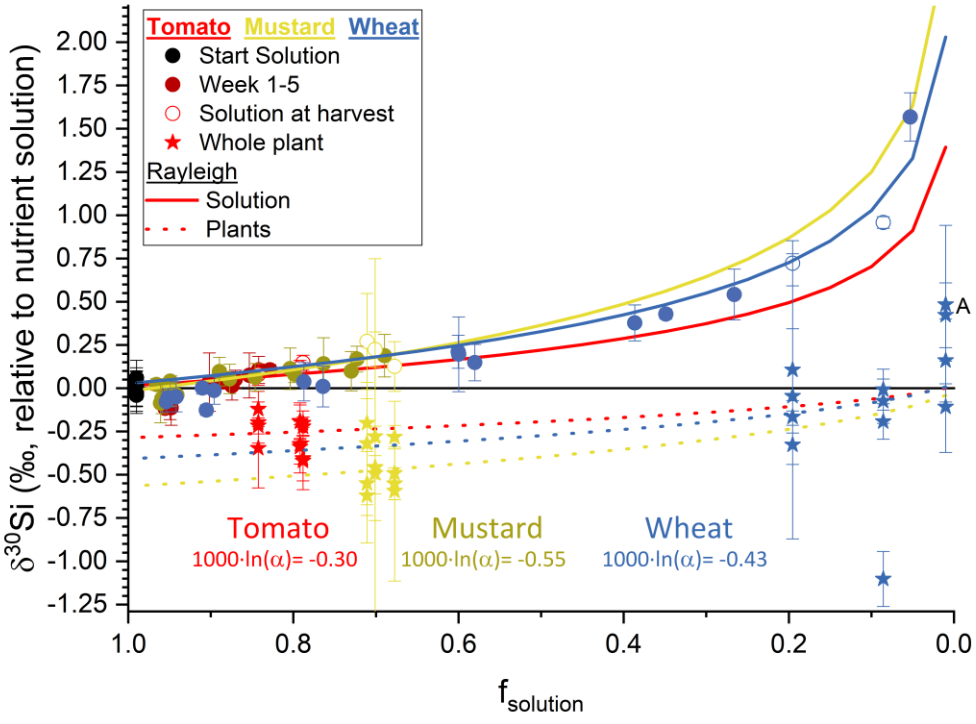

Figure 3: The silicon isotope composition (expressed in δ^{30}Si ‰ relative to nutrient solution) versus the amount of silicon taken up by the plants (expressed as dimensionless $f_{solution}$) (dots represents the nutrient solution, tomato in red, mustard in yellow and wheat in blue, starting solutions in black). Red, yellow and blue solid lines represent the best fit through a Rayleigh-like fractionation for the remaining solution, the dotted line the accumulated silicon isotope composition in the plants. Stars are the mass-weighted average isotopic composition of the individual plants at the respective $f_{solution}$ of the container at harvest. Plant samples denoted with A have no corresponding solution value, since the concentration of silicon was below the amount required for an isotope ratio determination. Uncertainty bars are based on two standard deviations.

https://doi.org/10.5194/bg-2020-66
Preprint. Discussion started: 9 April 2020

Tables

Parameter		Plant species		
		Mustard	**Wheat**	**Tomato**
Dry matter [g pot^{-1}]	Root	3.9 ± 1.1	2.6 ± 0.6	1.7 ± 0.2
	Shoot	25.0 ± 4.2	13.7 ± 2.0	10.3 ± 1.5
	Total plant	29.0 ± 5.2	16.3 ± 2.5	12.0 ± 1.7
Plant Si content [mg Si g^{-1} dry matter]	Root	8.6 ± 4.3	2.5 ± 2.8	3.5 ± 1.8
	Shoot	1.0 ± 0.3	24.2 ± 6.3	1.4 ± 0.7
	Total plant	2.0 ± 0.4	20.9 ± 4.0	1.3 ± 0.2
Plant Si uptake [mg Si pot^{-1}]	Root	31.1 ± 4.8	5.8 ± 3.1	4.1 ± 1.3
	Shoot	26.1 ± 3.8	331.3 ± 70.1	11.4 ± 3.6
	Total plant	57.2 ± 1.3	337.0 ± 67.9	15.5 ± 4.9
Transpiration [L pot^{-1}]	Pot	11.0 ± 0.3	6.8 ± 1.5	3.2 ± 0.6

Table 1: Dry matter, plant Si content, plant Si uptake and water transpiration of mustard, wheat and tomato after 6 weeks (hydroponic culture; mean ± standard deviation based on 3 pots with 4 plants each).

620

Quotient	Plant species		
	Mustard	**Wheat**	**Tomato**
Dry mass ratio [g shoot g^{-1} root]	6.5 ± 0.7	5.4 ± 0.9	5.9 ± 0.2
Si mass ratio [mg Si in shoot mg^{-1} Si in root]	0.9 ± 0.2	72.7 ± 47.8	2.7 ± 0.2
Water use efficiency [g L^{-1}]	2.6 ± 0.5	2.4 ± 0.2	3.8 ± 0.3
Si uptake efficiency [mg plant Si L^{-1}]	5.2 ± 0.3	50.3 ± 8.8	4.8 ± 0.6
Si transfer efficiency [mg shoot Si L^{-1}]	2.4 ± 0.3	49.3 ± 8.4	3.5 ± 0.4
Uptake classification (measured / theoretical Si uptake)	0.12±0.01	1.9±0.6	0.11±0.04

Table 2: Ecophysiological performance ratios for mustard, wheat and tomato (means ± standard deviation based on 3 pots with 4 plants each). The uptake classification is based on the ratio of measured and theoretical Si uptake. A ratio of greater than 1 indicates an active uptake mechanism, a ratio much smaller than 1 a rejective strategy and a ratio of 1 is passive uptake.

https://doi.org/10.5194/bg-2020-66
Preprint. Discussion started: 9 April 2020

Biogeosciences Discussions Open Access EGU

		Mustard			Wheat			Tomato		
	[mg]	Pot 1	Pot 4	Pot 7	Pot 2	Pot 5	Pot 8	Pot 3	Pot 6	Pot 9
Si	m_{Start}	418	421	399	425	416	411	418	415	414
	m_{End}	283	299	280	36	2	80	329	329	349
	m_{Plants}	58	56	58	299	415	297	20	15	11
	Retrieval	82%	84%	85%	79%	100%	92%	84%	83%	87%
Ca	m_{Start}	544	543	524	548	542	541	549	542	543
	m_{End}	3	0	0	382	376	423	139	182	264
	m_{Plants}	393	394	352	108	119	87	304	241	222
	Retrieval	73%	73%	67%	89%	91%	94%	81%	78%	90%
Fe	m_{Start}	39	39	38	39	40	39	39	39	39
	m_{End}	26	29	28	27	25	28	24	24	28
	m_{Plants}	4	4	3	6	4	3	5	5	2
	Retrieval	76%	85%	82%	85%	73%	80%	73%	75%	78%
K	m_{Start}	1787	1813	1742	1817	1801	1801	1803	1809	1801
	m_{End}	657	424	174	539	505	787	941	1044	1213
	m_{Plants}	1085	1218	1500	1556	1449	979	872	727	673
	Retrieval	98%	91%	96%	115%	109%	98%	101%	98%	105%
Mg	m_{Start}	121	121	116	122	120	119	122	121	120
	m_{End}	7	1	0	63	59	67	35	41	55
	m_{Plants}	82	95	73	30	26	27	52	55	33
	Retrieval	74%	79%	63%	76%	70%	80%	72%	79%	74%
P	m_{Start}	173	176	171	177	175	176	176	177	177
	m_{End}	5	2	1	0	0	11	5	20	52
	m_{Plants}	121	134	115	137	142	144	117	123	82
	Retrieval	73%	77%	68%	77%	81%	88%	69%	81%	76%
S	m_{Start}	180	183	174	182	182	182	183	182	182
	m_{End}	4	3	6	97	101	119	81	89	113
	m_{Plants}	95	88	73	61	57	33	60	55	38
	Retrieval	55%	50%	45%	87%	87%	84%	77%	79%	83%

Table 3: Major element budget for mustard, tomato and wheat. m_{Plants} is calculated based on the concentration of the element in the plant digest and the dry mass, the m_{Start} m_{End} are the element masses in mg based on the amount of nutrient solution and the element concentration at the start and the end of the experiment. Retrieval is the ratio between m_{Start} and the sum of m_{Plants} and m_{End}. The initial amount of the elements in the seeds, taken up during germination and the amount of element discharged in the wash water are not considered.

https://doi.org/10.5194/bg-2020-66
Preprint. Discussion started: 9 April 2020

	$\delta^{30}Si$	2 s	$\delta^{30}Si$	2 s	$\delta^{30}Si$	2 s
Mustard						
	Pot 1		Pot 4		Pot 7	
Start	-0.23	0.12	-0.19	0.06	-0.15	0.06
End	-0.20	0.30	-0.04	0.38	-0.09	0.26
Wheat						
	Pot 2		Pot 5		Pot 9	
Start	-0.18	0.03	-0.18	0.13	-0.24	0.07
End	-0.39	0.30	0.05	0.23	-0.12	0.27
Tomato						
	Pot 3		Pot 6		Pot 9	
Start	-0.20	0.08	-0.25	0.10	-0.23	0.02
End	-0.09	0.19	-0.11	0.31	-0.14	0.31

Table 4: Silicon isotope budget (calculated using Eq. (4)) for mustard, wheat and tomato at the start of the experiment (based on the isotopic composition of the nutrient solution) and the end (based on the plants and nutrient solution isotopic composition).

best fit	**Mustard**	**Tomato**	**Wheat**	**All data**
1000·ln(α) [‰]	-0.55 ± 0.40	-0.33 ± 0.32	-0.43 ± 0.09	-0.43 ± 0.09

Table 5: $^{30}Si/^{28}Si$ isotope fractionation factor 1000·ln(α) numerically approximated by reducing root-mean-square-deviation ('best fit') using Eq. (5) and uncertainties (1 s) from Monte Carlo method with n=500 seeded individual data sets.